

CONF-970744-

NONLINEAR FITTING OF ABSORPTION EDGES IN K-EDGE DENSITOMETRY SPECTRA

Michael Collins and Sin-Tao Hsue

Los Alamos National Laboratory

Safeguards Science and Technology Group, NIS-5 MS E540

Los Alamos, NM 87545 USA

RECEIVED

NOV 03 1997

OSTI

MASTER

*presented at the
Institute of Nuclear Materials Management
38th Annual Meeting
Phoenix, Arizona
July 20-24, 1997*

~~DISTRIBUTION OF THIS DOCUMENT IS UNLIMITED~~



Los Alamos
NATIONAL LABORATORY

Photograph: by Chris J. Lindberg

DISCLAIMER

**Portions of this document may be illegible
in electronic image products. Images are
produced from the best available original
document.**

DISCLAIMER

This report was prepared as an account of work sponsored by an agency of the United States Government. Neither the United States Government nor any agency thereof, nor any of their employees, makes any warranty, express or implied, or assumes any legal liability or responsibility for the accuracy, completeness, or usefulness of any information, apparatus, product, or process disclosed, or represents that its use would not infringe privately owned rights. Reference herein to any specific commercial product, process, or service by trade name, trademark, manufacturer, or otherwise does not necessarily constitute or imply its endorsement, recommendation, or favoring by the United States Government or any agency thereof. The views and opinions of authors expressed herein do not necessarily state or reflect those of the United States Government or any agency thereof.

NONLINEAR FITTING OF ABSORPTION EDGES IN K-EDGE DENSITOMETRY SPECTRA*

Michael Collins and Sin-Tao Hsue

Los Alamos National Laboratory

Safeguards Science and Technology Group, NIS-5 MS E540

Los Alamos, NM 87545 USA

Abstract

A new method for analyzing absorption edges in K-Edge Densitometry (KED) spectra is introduced. This technique features a nonlinear function that specifies the empirical form of a broadened K-absorption edge. Nonlinear fitting of the absorption edge can be used to remove broadening effects from the KED spectrum. This allows more data near the edge to be included in the conventional KED fitting procedure. One possible benefit is enhanced precision of measured uranium and plutonium concentrations. Because no additional hardware is required, several facilities that use KED may eventually benefit from this approach. Applications of nonlinear KED fitting in the development of the Los Alamos National Laboratory (LANL) hybrid K-edge/x-ray fluorescence (XRF) densitometer system are described.

Introduction

In the K-edge densitometer subsystem of the LANL hybrid K-edge/x-ray fluorescence instrument, a continuous-energy x-ray beam is shone through a glass vial containing a liquid sample. If the sample contains more than a few grams per liter of uranium, a uranium K-edge can be observed in the transmitted portion of the x-ray beam. The KED analytical software determines the transmission above and below the edge by linear fitting, from which the uranium concentration can be calculated.¹

Data points in the vicinity of the measured K-edge must be excluded from conventional KED analysis, which relies on linear fitting above and below the edge. Observed data near the edge have a complicated structure because of broadening effects within the detector. In this study, a nonlinear function that describes the empirical form of the broadened K-edge is derived. Edge shape parameters are determined by a nonlinear fitting routine that includes all data points near the edge. Nonlinear fitting of measured transmission data near the K-edge has two useful applications. First, a realistic edge shape can be incorporated in simulated KED spectra. Second, measured edges can be "sharpened" to allow more data points near the edge to be used in conventional KED fitting.

K-Absorption Edge

The K-absorption edge of uranium is found at an energy of 115.606 keV.² A photon with energy greater than E_K can interact photoelectrically with a uranium K electron. This causes a sharp increase in the mass attenuation coefficient of uranium at the K-edge energy. This edge can be observed in the measured KED spectrum as a steep decline in measured count rate with increasing energy in the 115 to 116 keV range (Fig. 1). The measured count rate is lower above E_K because the mass attenuation coefficient of uranium is higher above the edge.

*This work is supported by the US Department of Energy, Office of Nonproliferation and National Security, Office of Safeguards and Security.

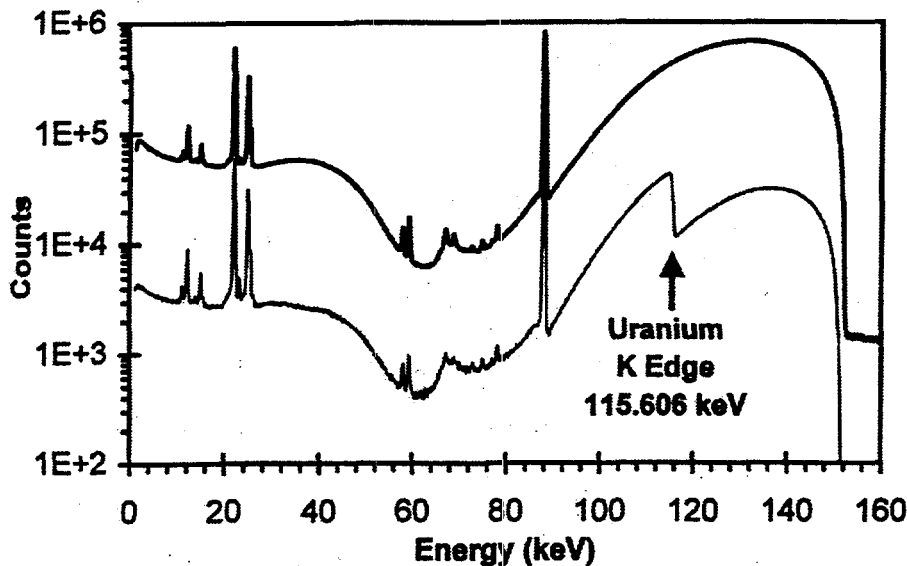


Fig. 1. Comparison of Measured KED Spectra. Top trace shows spectrum obtained with blank sample (3.0 molar nitric acid). Lower trace shows spectrum observed with uranium sample (200-g/L uranium dissolved in 3.0 molar nitric acid). The K-edge of uranium is clearly visible in lower trace.

A graph of the theoretical mass attenuation coefficient (μ) of uranium between 100 and 150 keV resembles a sharp sawtooth shape when plotted in $\ln(\mu)$ vs $\ln(E)$ space (Fig. 2). The empirical $\ln(\mu)$ decreases linearly in the region below $\ln(E_K)$. At $\ln(E_K)$ there is a sharp increase in $\ln(\mu)$. Above $\ln(E_K)$, $\ln(\mu)$ also decreases linearly, with a shallower slope than that observed below the edge. In this study, the theoretical form of the uranium K-edge was assumed to be that of a perfectly sharp sawtooth. Also, any fine structure effects near the absorption edge were assumed to be negligible.³

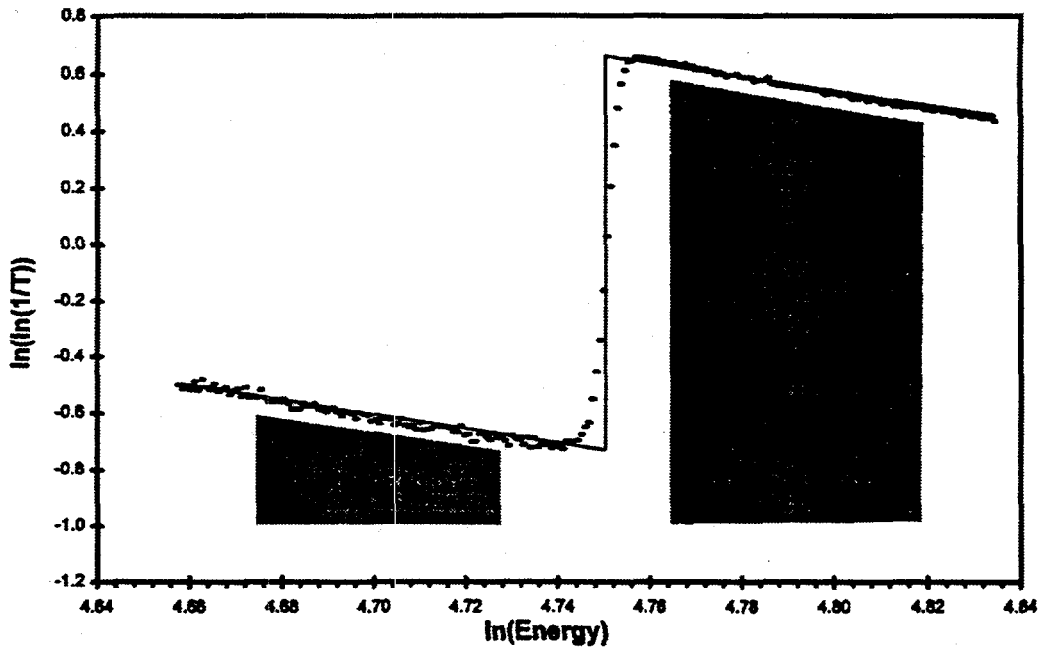


Fig. 2. Theoretical $\ln(\mu)$ and Measured $\ln(\ln(1/\text{Transmission}))$ plotted vs $\ln(\text{Energy})$. The solid line shows the logarithm of the theoretical mass attenuation coefficient of uranium. Black ovals illustrate measured $\ln(\ln(1/\text{Transmission}))$ values. Gray trapezoids indicate linear fitting regions for conventional KED analysis.

Traditional single-element K-edge densitometry analysis involves linear fitting of measured KED data in $\ln(\ln(1/\text{Transmission}))$ vs $\ln(\text{Energy})$ space. In the remainder of this paper, T will be used as the mathematical notation for transmission, and E represents energy. Fitting is performed in $\ln(\ln(1/T))$ vs $\ln(E)$ space because $\ln(\ln(1/T))$ is the same as $\ln(\text{Mu})$ plus a constant. Therefore, the measured $\ln(\ln(1/T))$ values exhibit a sawtooth shape similar to that described above for the theoretical $\ln(\text{Mu})$ values. However, the measured absorption edge is not perfectly sharp (see Fig. 2). The observed edge is curved because of finite resolution, and tailing effects, within the KED detector.

Unbroadened Transmission

In nonlinear KED fitting, it is advantageous to define transmission functions in terms of "channel position" instead of energy. The rationale for adopting this convention is as follows. The nonlinear KED fitting technique calculates the exact position of the K-edge in the measured data. The K-edge will probably not be observed at the exact channel position that the energy calibration would predict. It would be misleading to state that the edge (with known energy E_K) was observed at an energy other than E_K . It is more straightforward to state that the edge was observed at channel Ch_K . The channel position of the edge can be used to fine-tune the energy calibration. The new energy calibration is used to recalculate the mass attenuation coefficient of uranium for each channel.

The shape of the unbroadened K-edge in $\ln(\ln(1/T))$ vs $\ln(\text{Channel})$ space can be characterized with five parameters. They are described as follows:

- Ch_K = Position of the K-edge (in channels),
- A_L = $\ln(Ch_K)$ -intercept of data on left side of edge ,
- A_R = $\ln(Ch_K)$ -intercept on right side of edge,
- B_L = Slope of data on left side of edge, and
- B_R = Slope of data on right side of edge.

These five parameters are also used to characterize the more complicated shape of the unbroadened K-edge in Transmission vs Channel space.

The unbroadened transmission T_{unbr} is obtained by mapping the linear functions for $[\ln(\ln(1/T))$ vs $\ln(Ch)$] above and below the K-edge into Transmission vs Channel space:

$$T_{\text{unbr}}(Ch) = \begin{cases} T_{\text{Left}}, & Ch \leq Ch_K \\ T_{\text{Right}}, & Ch > Ch_K \end{cases} , \quad (1)$$

where $T_{\text{Left}}(Ch) = \frac{1}{\exp(\exp(A_L + B_L[\ln(Ch) - \ln(Ch_K)]))}$,

and $T_{\text{Right}}(Ch) = \frac{1}{\exp(\exp(A_R + B_R[\ln(Ch) - \ln(Ch_K)]))}$.

T_{unbr} describes the functional form of measured transmission values in the absence of broadening effects. $T_{\text{unbr}}(Ch)$ is proportional to the predicted rate at which x-rays of energy $E(Ch)$ interact with the KED detector.

It is worthwhile to note that T_{Left} and T_{Right} are not linear in Transmission vs Channel space. However, the following expression is a very good approximation for unbroadened transmission near the absorption edge:

$$T_{unbr}(Ch) = \begin{cases} T_L + k_L(Ch - Ch_K), & Ch \leq Ch_K \\ T_R + k_R(Ch - Ch_K), & Ch > Ch_K \end{cases}, \quad (2)$$

where

$$T_L \equiv T_{Left}(Ch_K),$$

$$k_L \equiv \left(\frac{\partial T_{Left}}{\partial Ch} \bigg|_{Ch_K} \right),$$

$$T_R \equiv T_{Right}(Ch_K), \text{ and}$$

$$k_R \equiv \left(\frac{\partial T_{Right}}{\partial Ch} \bigg|_{Ch_K} \right).$$

This linear approximation for T_{unbr} near the edge will be used later in calculating the broadened transmission.

Broadening Function

In order to determine the form of the broadened edge, a broadening function must be applied to the unbroadened edge. The broadening function specifies the shape of the detector's response to a monoenergetic source. The broadening function used in this study is a composite that includes two significant components of peak shape.

The response of a high-resolution germanium detector to a monoenergetic source can be sufficiently characterized as the sum of three functions.⁴ The most prominent of these is the Gaussian distribution of counts, with centroid at channel Ch_0 and width parameter s . Next in significance is the empirical short-term tailing component, which is manifested only in channels below the centroid. The short-term tail reaches its maximum height just below Ch_0 and tapers off steeply on the low energy side.

A third component is the background continuum, which can be approximated as a uniform step in channels below Ch_0 . The height of the step background is a scalar multiple of the height of the Gaussian peak. The ratio of peak height to step background height depends upon the energy of the peak. In KED analysis, the background continuum is subtracted from both the measured and reference spectra before transmission values are calculated. Fitting is performed on background-subtracted transmission values, so there is no need to include a term for background continuum in the broadening function.

Because the fitting region is only a few keV wide, all broadening parameters are evaluated near the K-edge and are assumed to be constant. For ease in calculation, it was useful for the area underneath the broadening basis functions to be normalized to unity. Calculations were simplified by using dimensionless variables, so that extensive use could be made of the normal probability density function and its integral.⁵ All channel positions were expressed relative to the K-edge in terms of a dimensionless parameter z :

$$z = \left(\frac{Ch - Ch_K}{\sigma} \right), \quad (3)$$

where Ch = Channel position of interest,
 Ch_K = Channel position of K-edge, and
 σ = Gaussian width parameter (in channels).

All basis functions for detector response shown below, and their integrals, are defined in terms of this parameter z .

The basis function for the Gaussian broadening component is simply the normal probability density function:

$$G(z) = \frac{1}{\sqrt{2\pi}} \exp\left(-\frac{z^2}{2}\right), \quad (4)$$

The basis function for the short-term tail component is as follows:

$$S(z) = \begin{cases} \frac{1}{\lambda} \exp(bz) [1 - \exp(-cz^2)] & , z < 0 \\ 0 & , z \geq 0 \end{cases}, \quad (5)$$

where λ is the normalization factor for the short-term tail, b is the tailing slope, and c is the width parameter of the tail. The short-term tail basis function is normalized to unity in order to simplify intermediate calculations. Because $S(z)$ is normalized to unity, similar notation can be applied to all mathematical quantities involving the Gaussian and short-term tail components.

The cumulative broadening function $B(z)$ is simply the sum of weighted Gaussian and short-term tail basis functions:

$$B(z) = (1 - \gamma)G(z) + \gamma \cdot S(z), \quad (6)$$

where γ is the weight of the short-term tail component. The value of γ can be determined experimentally using a monoenergetic source. Gamma is the ratio of short-term tail area to the combined area of the Gaussian peak and short-term tail. It is worth noting that the cumulative broadening function $B(z)$ is itself normalized to unity. The cumulative broadening function is illustrated in Fig. 3, along with its weighted Gaussian and short-term tail components.

Broadened Transmission

Now that the cumulative broadening function is defined, it can be applied to the unbroadened transmission to obtain the functional form of the broadened transmission. This will be determined as a function of channel position Ch . The broadened transmission at any channel position Ch is proportional to the background subtracted count rate observed at that channel.

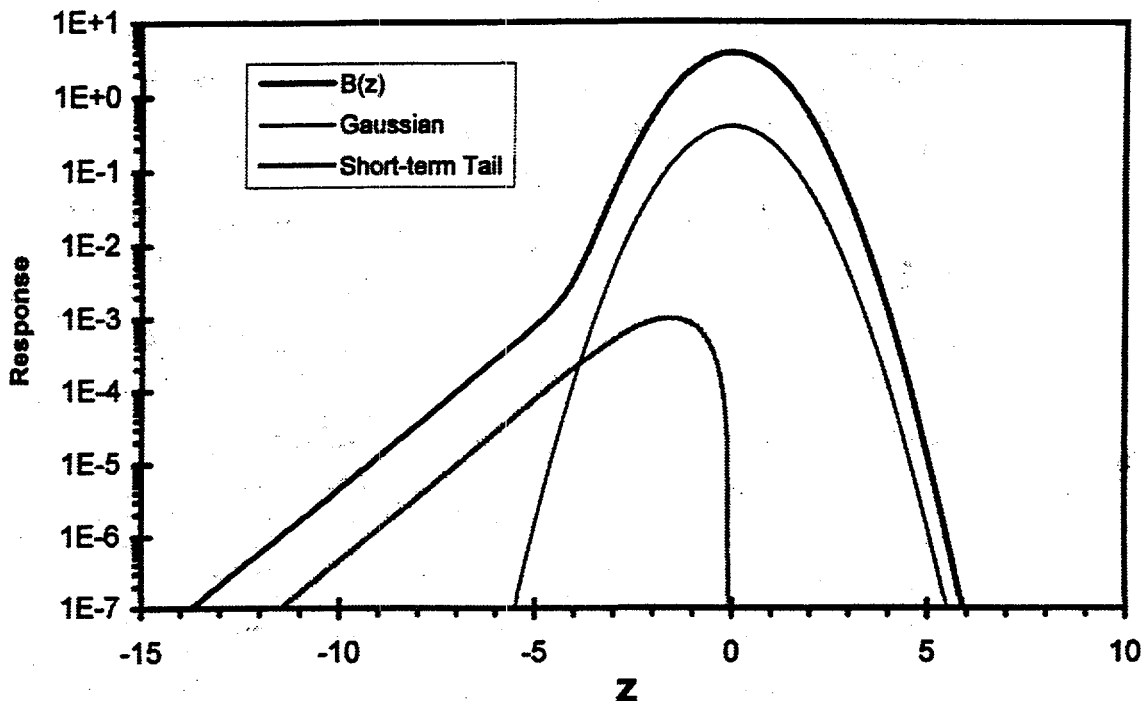


Fig. 3. Cumulative broadening function, shown with weighted Gaussian and short-term tail components. In this plot, $b=1.02$, $c=0.2$, and $\gamma=0.032$. The cumulative broadening function was multiplied by a factor of 10 for illustrative purposes.

The rate at which incident x-rays of energy $E(Ch')$ are fully absorbed by the detector is proportional to the unbroadened transmission T_{unbr} at channel Ch' . In the absence of broadening effects, every event that deposits energy $E(Ch')$ would be counted in channel Ch' . With a perfect detector, we would measure a sharp edge with transmission profile that matched T_{unbr} .

Because of broadening effects, a fraction of the events that would otherwise have been observed in channel Ch' are actually counted in channel Ch . Suppose that the width of each channel is infinitesimal. The count rate observed at channel Ch is the integral of the count rate contributions to Ch from all neighboring channels:

$$T_{br}(Ch) = \int_{Ch'=-\infty}^{\infty} T_{unbr}(Ch') \frac{1}{\sigma} B\left(\frac{Ch - Ch'}{\sigma}\right) dCh' . \quad (7)$$

The resulting broadened transmission function is

$$T_{br}(Ch) = \left\{ T_L + k_L \sigma(z - A_{ZB}) + I_{ZB} \sigma(k_L - k_R) + I_B [(T_R - T_L) + \hat{U} z (k_R - k_L)] \right\} , \quad (8)$$

where $I_B(z) = \int_{z=-\infty}^z B(z') dz'$,

$I_{ZB}(z) = \int_{z=-\infty}^z z' B(z') dz'$, and

$$A_{ZB} = \lim_{z \rightarrow \infty} [I_{ZB}(z)].$$

This function T_{br} is derived from basic principles of edge structure and detector response and describes the predicted form of broadened transmission near the absorption edge.

Nonlinear Fitting

The goal in nonlinear absorption edge fitting is to determine the vector \bar{X} that minimizes the following chi-squared function:

$$\chi^2(\bar{X}) = \sum_{Ch=Ch_{Min}}^{Ch_{Max}} [T_{br}(Ch, \bar{X}) - T_{meas}(Ch)]^2, \quad (9)$$

where

$$\bar{X} = \begin{pmatrix} Ch_K \\ A_L \\ A_R \\ B_L \\ B_R \end{pmatrix}$$

is a vector that contains shaping parameters for the edge, Ch_{Min} is the lowest channel in the fitting region, and Ch_{Max} is the highest channel in the fitting region. The Gaussian width parameter s and short-term tail parameters b , c , and γ are calculated experimentally and provided as input to the solver.

In this technique, the parameters of a perfectly sharp edge are deduced from measured transmission values. In effect, inverse broadening is performed. The solution describes the unbroadened edge that is consistent with both the measured edge and the known broadening function.

A prototype FORTRAN code named EDGE_FIT was written to perform computations related to nonlinear fitting of the uranium K-edge. The nonlinear least-squares solver routine SNLS1 from the MINPACK library was used to solve the above minimization problem.⁶ This routine incorporates the Levenberg-Marquardt algorithm, which performs unconstrained nonlinear least-squares minimization of the chi-squared function.⁷ The EDGE_FIT program features two modes of operation. In the first mode, a sharp edge is broadened. In the other mode, a broad edge is sharpened.

Broadening Mode

The first application of the EDGE_FIT program involves KED spectrum simulation. In KED simulation, the goal is to construct a realistic spectrum that corresponds to a given uranium concentration. A previously reported technique for KED spectrum simulation involved the use of tabulated mass attenuation coefficients to calculate transmission values. Because tabulated values

were used, this simulation technique resulted in a sharp edge.⁸ This was not a problem for the conventional KED analysis code, which does not use data near the edge in fitting. However, the sharp edges did not meet the goal of realism in simulated spectra. The simulated edges needed to be broadened in an authentic manner.

Operated in broadening mode, the EDGE_FIT program inputs an array of transmission values T_{input} that contains a sharp edge. The edge position Ch_k is located. Linear fitting is performed above and below the sharp edge to determine A_L , A_R , B_L , and B_R . Broadening parameters σ , b , c , and γ are read from a parameter file. The data in each channel is broadened according to the following function:

$$T_{\text{output}}(Ch) = T_{\text{input}}(Ch) + [T_{br}(Ch) - T_{unbr}(Ch)]. \quad (10)$$

The EDGE_FIT program outputs this array of broadened transmission values to the KED simulation program. These values are scaled, Compton continuum is added, and statistical fluctuations are incorporated. The result is a simulated KED spectrum that appears decidedly real (see Fig. 4).

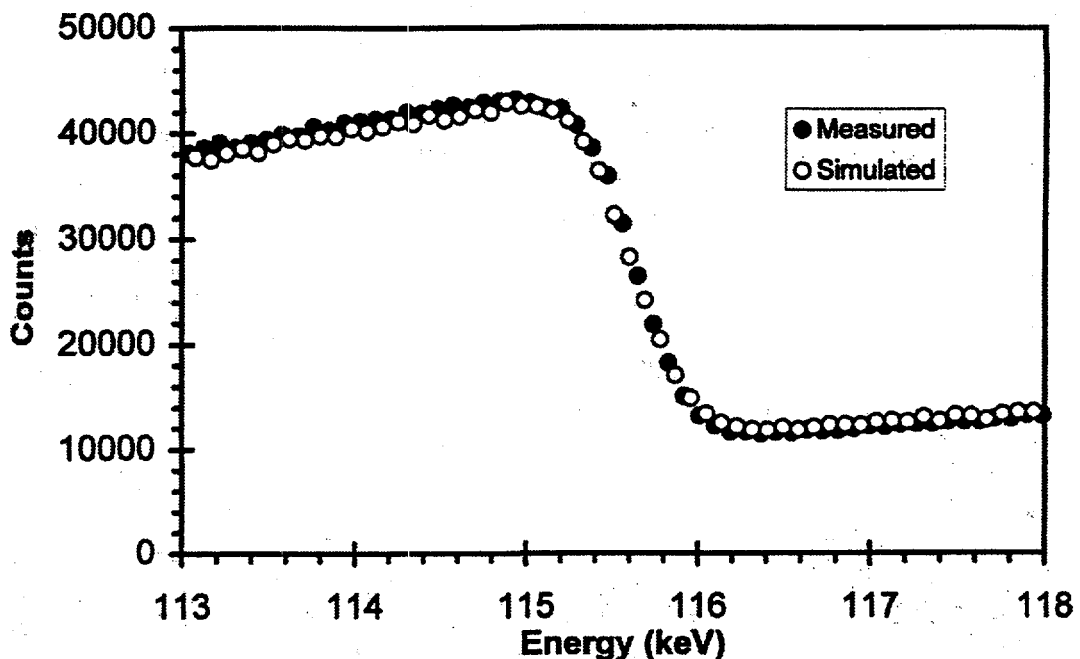


Fig. 4. Comparison of simulated and measured KED spectra. Solid circles show near-edge data obtained by measuring a 200-g/L uranium solution. Hollow circles show simulated spectrum for same solution using the new edge-broadening technique.

Sharpening Mode

The other feature of the EDGE_FIT program is K-edge sharpening. In this mode, the program removes broadening effects from an array of measured transmission values. Nonlinear KED fitting is performed on the measured transmission values. The solution vector describes the empirical broadened transmission function that best fits the measured data.

The difference between the empirical broadened and unbroadened transmission functions indicates the deviation of measured data from the shape of a perfectly sharp edge. The data is sharpened by adding

the difference between the empirical functions for broadened and unbroadened edges to each measured transmission value near the edge. The sharpening adjustment is performed as follows:

$$T_{\text{sharp}}(Ch) = T_{\text{meas}}(Ch) + [T_{\text{unbr}}(Ch) - T_{\text{br}}(Ch)], \quad (11)$$

where T_{sharp} is the array of sharpened transmission data.

The sharpened edge contains the statistical fluctuations that were present in the measured transmission data (fig. 5). The unbroadened transmission function T_{unbr} is the empirical form of the sharpened data. The EDGE_FIT program outputs an array of sharpened transmission values, along with the observed channel position of the uranium K-edge.

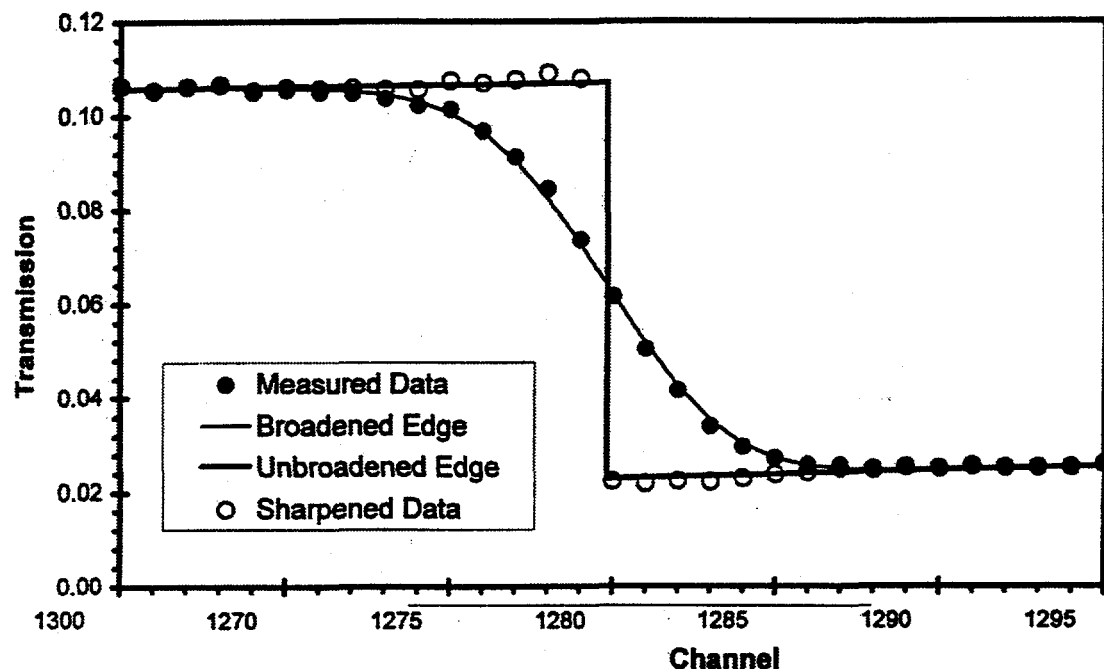


Fig. 5. Illustration of KED sharpening. Solid dots indicate measured transmission values. The thin line shows the broadened transmission function that was fitted to measured data using the nonlinear solver. The bold line illustrates the unbroadened transmission function. Hollow circles indicate sharpened transmission data.

The ability to sharpen absorption edges makes a new analytical technique possible for KED spectra. This technique would use KED sharpening in an effort to include more data near the edge in linear KED fitting. Measured transmission values are sharpened via the above-mentioned edge-sharpening procedure. Traditional single-element KED fitting is performed on the sharpened transmission data. However, the upper energy boundary of the lower fitting window is defined at an energy that is closer to the K-edge. The lower energy boundary of the upper fitting window is also moved closer to the edge. The wider fit windows result in the utilization of more data in KED fitting.

The inclusion of more data points near the edge enhances the theoretical precision of measured concentration values. With conventional KED fitting, the precision of the measured uranium concentration (for a 200-g/L uranium solution) is about 0.20%. With the inclusion of edge sharpening, the predicted precision for the same solution is 0.15%. Once the edge sharpening capability is incorporated into the hybrid KED/XRF analytical software, this prediction will be tested.

Conclusions

A closed-form expression was derived for the empirical form of a broadened K-absorption edge. The broadened transmission function provides insight into the detailed structure of a measured absorption edge. A nonlinear least-squares technique for fitting measured data to the broadened transmission function was presented. A FORTRAN program was written to perform two important tasks: edge broadening and edge sharpening. A new technique for analyzing single-element KED spectra was proposed.

The next step in the study of nonlinear KED fitting is to add the option of edge sharpening to the hybrid K-edge/XRF densitometer analytical software. This will allow the effect of edge sharpening on precision to be measured. The optimal boundaries of linear and nonlinear fitting windows will need to be determined. KED sharpening will also be applied to spectra containing multiple absorption edges.

References

1. H. Ottmar and H. Eberle, "The Hybrid K-Edge/K-XRF Densitometer: Principles - Design - Performance," Kernforschungszentrum Karlsruhe, Germany, KfK 4590, February 1991, pp. 15-20.
2. E. Storm and H. I. Israel, "Photon Cross Sections from 1 keV to 100 MeV for Elements Z=1 to Z=100," Nuclear Data Tables A7 (1970), pp. 565-642, RSIC Data Library Collection DLC-15, Oak Ridge, Tennessee.
3. M. Nomura, "XAFS Applied to Trace Element Analysis," *Japan J. Appl. Phys.* Vol 32 Suppl. 32-2, pp. 237-9 (1993).
4. R. Gunnink, W. D. Ruhter, and J. B. Niday, "GRPANL: A Suite of Computer Programs for Analyzing Complex Ge and Alpha-Particle Detector Spectra." Lawrence Livermore National Laboratory report UCRL-53861, Vol. 1 (May 1988), pp. 7-8.
5. M. Abramowitz and I. E. Stegun, "Handbook of Mathematical Functions," Applied Mathematics Series, Vol. 55, National Bureau of Standards. (Government Printing Office, Washington DC, 1972) pp. 927-33.
6. J. J. More, B. S. Garbow, and K. E. Hillstrom, "User Guide for MINPACK-1," Argonne National Laboratory report ANL-80-74 (1980).
7. W. H. Press, et. al., "Numerical Recipes (FORTRAN version)," (Cambridge University Press, New York, 1989) pp. 523-528.
8. S. T. Hsue and M. L. Collins, "Simulation of Absorption Edge Densitometry," Los Alamos National Laboratory manuscript LA-12874-MS (November 1994).